Appl Phys A (2009) 94: 657–665
DOI 10.1007/s00339-008-4896-1

Applied Physics A
Materials Science & Processing

Laser ablation of energetic polymer solutions: effect of viscosity and fluence on the splashing behavior

Romain Fardel · Lukas Urech · Thomas Lippert · Claude Phipps · James M. Fitz-Gerald · Alexander Wokaun

Received: 5 May 2008 / Accepted: 3 September 2008 / Published online: 26 September 2008

Abstract Laser plasma thrusters are a new kind of propulsion system for small satellites, and work with the thrust created by the laser ablation of a target. Liquid polymer solutions are very promising fuels for such systems, provided that no splashing of the target occurs, because ejection of droplets strongly decreases the performances of the system. We have investigated the nanosecond infrared laser ablation of glycidyl azide polymer solutions containing carbon nanoparticles as absorber. Shadowgraphy imaging revealed two cases, namely splashing regime and solid-like behavior. The transition between both regimes depends on the viscosity of the solution and on the laser fluence, and is explained by the recoil force acting on the target. Appropriate conditions to avoid splashing were identified, showing that this liquid polymer solution is a suitable fuel for laser plasma thrusters.

PACS 52.38.Mf · 52.75.Di · 07.87.+v

R. Fardel
Laboratory for Functional Polymers, Empa, Swiss Federal Laboratories for Materials Testing and Research, Überlandstrasse 129, 8600 Dübendorf, Switzerland

R. Fardel · L. Urech · T. Lippert (✉) · A. Wokaun
General Energy Research Department, Paul Scherrer Institut, 5232 Villigen PSI, Switzerland
e-mail: thomas.lippert@psi.ch

C. Phipps
Photonic Associates, LLC, 200A Ojo de la Vaca Road, Santa Fe, NM 87508, USA

J.M. Fitz-Gerald
Department of Materials Science & Engineering, University of Virginia, 395 McCormick Road, Charlottesville, VA 22904-4745, USA

1 Introduction

Micro-satellites for space applications allow to perform new tasks at reduced cost compared to conventional satellites (>100 kg). Due to their low mass, these satellites have special issues regarding the propulsion system. The main requirements are a high specific impulse and precise control of the thrust intensity, which are not fulfilled by conventional rocket thrusters. Therefore, there is a need to design novel systems for space micropropulsion. One suitable technology for this purpose is the laser plasma thruster, where the impulse is provided by laser ablation [1–7]. An infrared diode laser is focused onto a transparent ribbon coated with an energetic material, which is ablated by the laser pulse. The so-created plasma provides the thrust to propel the satellite along one axis. After each pulse, the ribbon is moved forward similar to an audio tape. Energetic polymers are ideal target materials, because of their high energy density and low thermal conductivity, yielding precise ablation [8]. Among them, the glycidyl azide polymer (GAP) doped with an infrared absorber (carbon nanoparticles) is an excellent candidate for this purpose, with a specific impulse up to 860 s and efficiency up to 360% [9]. This high number is necessary for this application and shows clearly that the laser plasma thruster is actually a hybrid system, i.e., energy comes from both the laser and the material.

The main disadvantage of this design is the use of a tape as fuel dispenser, which limits the mass of fuel on board the satellite, but also induces undesirable angular momentum due to the rotation of reels. The alternative is to use liquid fuels, stored in a tank, with a good energy density and dispensed according to the needs. A solution of polymer is pumped through a nozzle, where it forms the target. After laser ablation, the target droplet is renewed by pumping again. Apart from the above-mentioned advantages, this

Table 1 Composition and viscosity of the solutions

Sample	Weight content			Viscosity
	GAP	CNP	EA	[Pa s]
0% GAP	0%	1%	99%	
1% GAP	1%	1%	98%	
28% GAP	28%	1%	71%	0.012
50% GAP	50%	1%	49%	0.46
70% GAP	70%	1%	29%	14

system works in reflection mode, i.e., the thrust direction is facing the incident laser beam. This allows a smooth transition from low to high impulse with the same configuration, different to the tape system, where the laser intensity is transmitted through and attenuated by the tape.

Obviously, the solution has to be liquid enough to be pumped easily through the nozzle. On the other hand, previous works have shown that the ablation of liquid targets yields very low specific impulse [10, 11], for instance 19 s with carbon-ink-doped water [12]. This is essentially due to the splashing of the liquid, which drives out the laser energy into droplet formation instead of high-velocity plasma acceleration. Moreover, splashing materials would contaminate the laser optics and compromise the reliability of the system, and energy stored in the energetic fuel would also be lost. Therefore, it is essential to find appropriate conditions under which the solution does not exhibit splashing if one wants to use liquid as fuel for laser plasma thrusters.

Laser ablation of liquids and liquid-containing materials has been investigated by several authors. The anisotropic structure of liquid as well as the weak intermolecular bonding make it an ideal model system for fundamental studies. For instance, liquid benzene ablation was investigated in this purpose by shadowgraphy [13, 14]. The ablation of water-based material, such as biological tissues, has also a big interest for biological and medical applications [15, 16].

In the present work, we have investigated five liquid solutions of GAP (including one without polymer) plus a solid GAP target by shadowgraphy to test if liquid polymer solutions are applicable and even superior to solid fuels in micro laser plasma thrusters. Shadowgraphy was used to test whether a fuel composition could be identified that would behave similar to solid GAP upon ablation, i.e., whether splashing can be avoided. We have also investigated the particle size distribution in the solutions by wet scanning electron microscopy (WSEM).

2 Experimental part

Glycidyl azide polymer (GAP) was obtained as 40 wt% solution in ethyl acetate (Nitrochemie, Wimmis, Switzerland). If required, a more concentrated solution was obtained by solvent evaporation under vacuum. Carbon nanoparticles (Black Pearls 2000) from Cabot were added as infrared absorber to obtain 1 wt% in the final sample. The carbon nanoparticles (CNP) were previously dispersed in the solvent with a high-performance homogeniser of the type Ultra-Turrax®. Solid GAP samples were prepared by adding a cross-linker (one drop of dibutyltin dilaurate and 13 wt% of hexamethylene-1,6-diisocyanate), solvent casting on a glass slide and drying in vacuum. The liquid samples were prepared by diluting GAP and CNP in ethyl acetate (EA), according to Table 1. The solutions were put as droplets with 1 cm diameter onto a polytetrafluoroethylene slide.

The targets were irradiated by the pump laser (Nd:YAG, $\lambda = 1064$ nm, $\tau = 6$ ns) focused by a lens on a circular spot of 300 µm diameter. For the solid sample, each pulse was directed onto a new sample position. For the liquids, special care was taken to refresh the droplet regularly to avoid its modification by laser irradiation. The illumination was obtained by a fluorescent dye pumped with the probe laser (XeCl excimer, $\lambda = 308$ nm, $\tau = 30$ ns). The delay between the pump and the probe pulse was set by a digital pulse/delay generator. A camera with a zoom objective was placed on the opposite side of the dye to image the process.

Viscosity measurements were performed with a rotational rheometer system (MCR 300, Paar-Physica) at a temperature of 20°C. A coaxial cylinder (GAP 28%) and a parallel-plate/plate cell (GAP 50 and 70%) were used.

Recently, vacuum encapsulation specimen holders were developed that allow direct imaging of wet samples in a scanning electron microscope (SEM) [17, 18]. Microscopy of the carbon dispersions was performed in a JEOL 6700F high-resolution SEM with solid state high-resolution backscatter electron detector (BSE) combined with energy dispersive X-ray analysis (EDX). Wet imaging capsules were purchased from Quantomix™ for imaging in a high vacuum environment [19, 20]. The capsules provide for a 16 µl sample well, separated from vacuum by a 100 nm thick Kapton® membrane. In operation, the primary electron beam passes through the membrane and interacts with the sample system, resulting in the ejection of backscattered electrons and characteristic X-rays. Imaging in wet SEM (WSEM) and chemical analysis are then accomplished through the detection of these events following scattering back through the membrane.

Thrust measurements were done with a torsion balance as described elsewhere [1, 6].

3 Results and discussion

3.1 Shadowgraphy imaging

Shadowgraphy was used to visualize the shock wave and the material ejection and to determine the conditions under

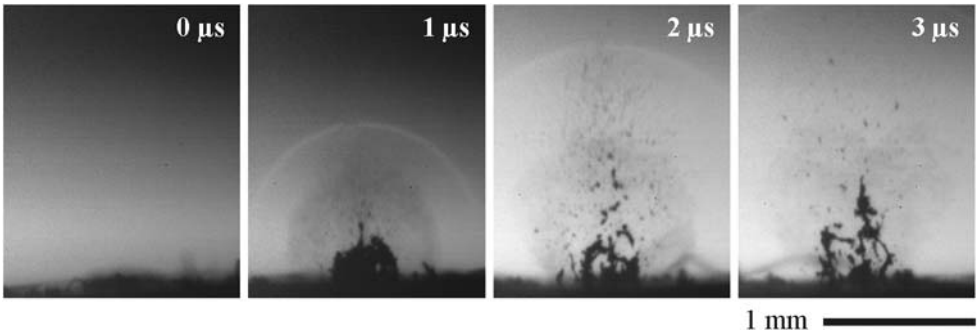

Fig. 1 Sequence of pictures taken for solid GAP at 3.2 J/cm^2

which droplet ejection can be avoided. The solid GAP and the solvent were first investigated to define the two limiting cases. Figure 1 shows the time evolution of an ablated film of solid GAP irradiated at 3.2 J/cm^2. The ablation of solid GAP + CNP targets produces a shock wave (visible at 1 and 2 µs) and the ejection of particles. At higher fluences (not shown), where a plasma is formed, particles cannot be observed due to the intense plasma emission. A performance similar to this behavior is the benchmark for the liquid polymers.

A shadowgraphy sequence of ablation of the 0% GAP solution at 2.8 J/cm^2 is presented in Fig. 2. The ablation of a liquid target (pure solvent with carbon) yields a different behavior than for the solid GAP. A cloud of droplets is ejected at first, but after several microseconds the liquid surface begins to collapse and produces a jet of liquid. This behavior, described as *splashing*, is still observed at timescales longer than 200 µs. This case is taken as a reference of the undesired behavior for a laser plasma thruster.

Having identified the two limiting cases, solutions of GAP at three different concentrations were investigated over a broad fluence range. Depending on polymer concentration and fluence, two possible behaviors are observed during the ablation of liquid GAP solutions. One case is shown in Fig. 3, recorded with a 70% GAP solution at 2.2 J/cm^2. Within 5 µs, the material is ablated and particles are ejected. Remaining particles or droplets are still ejected until 10 to 20 µs. After this time, the ablation process is finished. This process is comparable to the ablation of solid targets, although it differs on some features: the ejected material cloud appears more dense and more directed in the liquid target, and the particle front overtake the shock wave after 1–2 µs. This is not observed for solid GAP, where a less visible particle jet surrounds the dense core of large particles. However, the apparent difference in the particle velocity may only be an effect of the visibility of ejected material.

The other observed process is the removal of liquid material by splashing. Figure 4 shows the evolution during splashing of a 28% GAP target irradiated at 4.5 J/cm^2. The very first steps are similar to the nonsplashing ablation. However, two different features can be distinguished: liquid filaments are visible in the plume (which overtake the shock wave at 2 µs), and the base of the plume is connected to the liquid surface by a meniscus. This becomes particularly clear at 5 µs, where the liquid surface appears similar to a liquid after impact of a solid particle. The area of the moving liquid is much larger than the original spot size of 300 µm. After 20 µs the surface of the liquid seems to expand to several millimeters. After 500 µs (not shown) the liquid surface is still in an upward movement.

It appears that liquid GAP targets can exhibit both behaviors. The concentration of GAP and the applied fluence were varied to find their respective influence on the transition between the two regimes. Pictures taken after 10 µs were chosen to decide which of the processes is observed. The results are summarized in Fig. 5, where the fluence increases from left to right and the GAP concentration increases form top to bottom.

At low fluence (0.6 J/cm^2), all concentrations have the same "classical" behavior and no liquid is ejected at 10 µs. When increasing the fluence, the less viscous solutions start to produce splashing, first the 28% solution above 0.8 J/cm^2, then the 50% solution from 2.2 J/cm^2. The 70% GAP sample still reveals the nonsplashing behavior even at the highest applied fluence (7.5 J/cm^2), where plasma onset is observed (bright spot in the pictures) close to the laser–liquid interaction zone.

For a given concentration of GAP, there is a transition between the solid-like mode and the splashing mode when the fluence is increased. There is also a clear relation between the concentration of the solution and the fluence at which this transition occurs. The less concentrated the solution is, the lower this transition fluence is observed. For the 70% concentration, this transition is not observed in the investigated fluence range, showing that this solution behaves similar to solid GAP.

To quantify these results in more detail the viscosity of the solutions has been measured. As reported in Table 1, the three solutions have very different rheological properties, as the dynamic viscosity increases very fast for GAP concentrations >50%. It appears that the required viscosity to apply liquid GAP solution as fuel for micro laser plasma thruster is approximately above 10–15 Pa s.

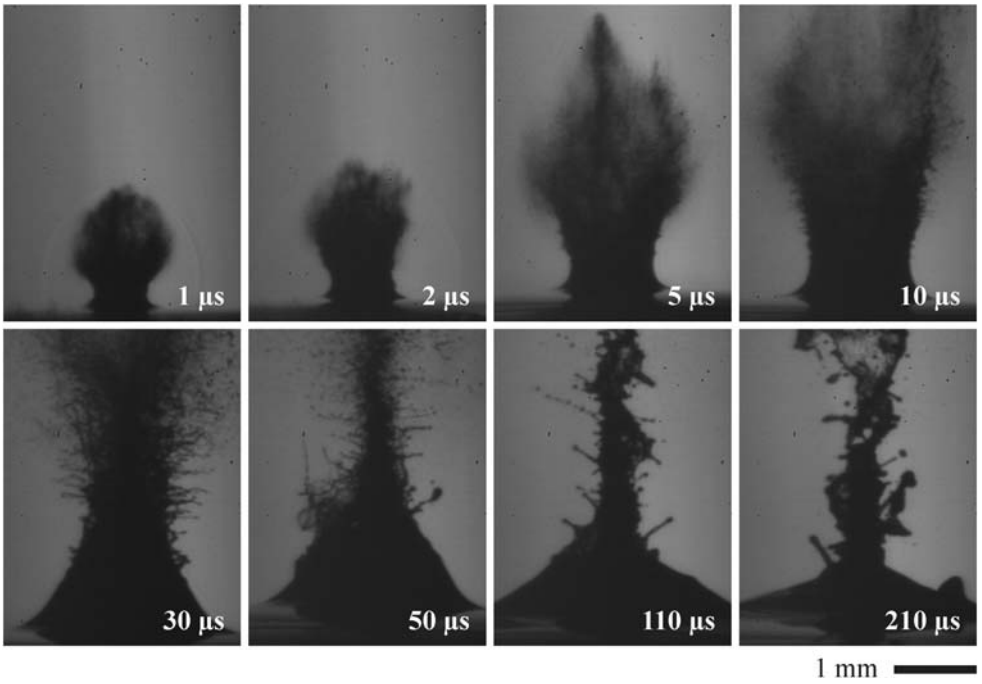

Fig. 2 Sequence of pictures taken for solvent (0% GAP solution) at 2.8 J/cm^2

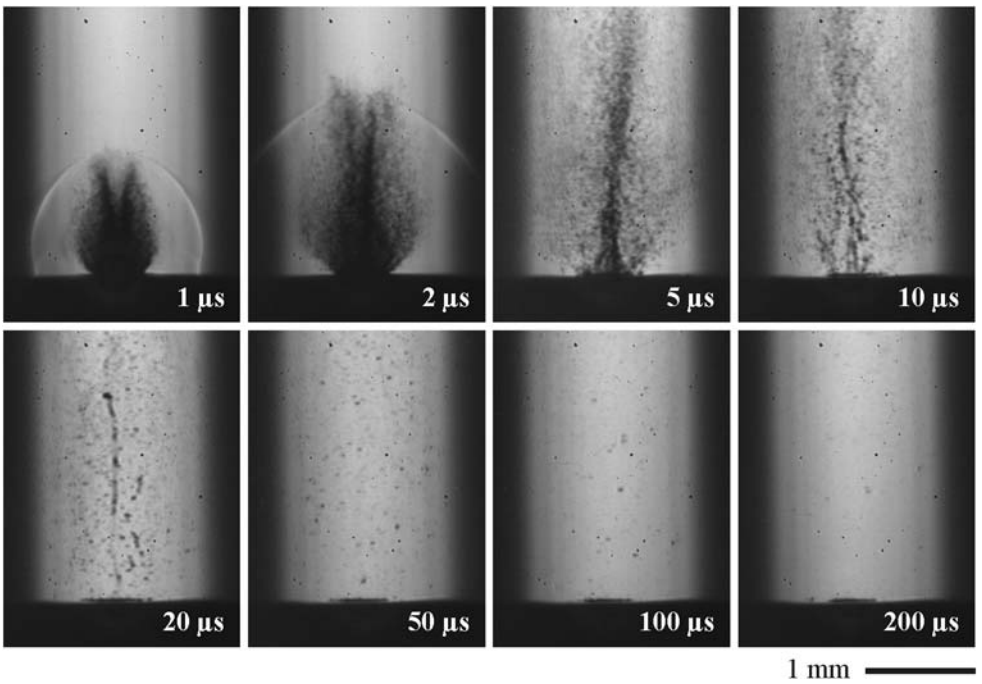

Fig. 3 Sequence of pictures taken for the 70% GAP solution at 2.2 J/cm^2, showing a solid-like ablation behavior

This clear influence of the viscosity on the splashing behavior have been observed by other groups as well. Hopp and coworkers have investigated the UV ablation of polyethylene glycol across the melting point [21]. They showed that splashing occured only above the melting point and attributed this fact to the change in the viscosity of the target. Apitz and coworkers have reported ablation of water and water-containing targets (biological tissues) at 2.94 µm [16] and have observed that, opposite to water, no splashing occured for mechanically strong materials such as skin. Viscosity cannot be considered for biological tissues, rather the resistance of the tissue to mechanical stress is important in this case.

The ablation of liquid targets can be described as follows. When a layer of material is removed by ablation, the recoil creates a hemispherical hole in the liquid surface, corresponding to radially outward material displacement. Due to the incompressibility of the liquid, material must be pushed

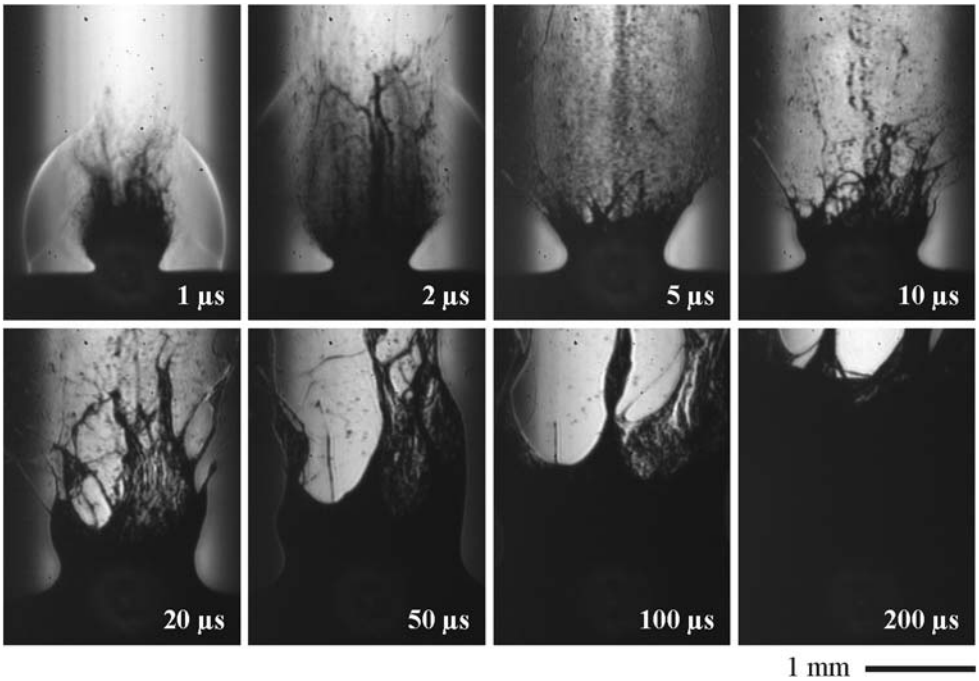

Fig. 4 Sequence of pictures taken for the 28% GAP solution at 4.5 J/cm^2, showing a splashing ablation behavior

away: liquid is ejected upward on the side of the hole and forms a jet, which eventually collapses after several tens of microseconds [16, 21]. The same phenomenon appears in the present work. For low viscosity solutions, a liquid jet is created by the displacement of the liquid surface. When the viscosity is high enough, the resistance of the liquid to movement prevents the recoil force to initiate the dynamic of liquid ejection. The effect of the fluence on the splashing is also clear: a higher fluence creates a stronger recoil, which eventually overcomes the liquid resistance at the fluence above which splashing is observed.

3.2 Shock wave evolution

From the shadowgraphy experiments, the evolution of the shock wave front can be measured as well. The position of the shock waves versus time is shown in Fig. 6 for the three solutions at 0.6 mJ/cm^2 and for the solid GAP at 1.5 mJ/cm^2.

All three solutions and the solid GAP show a similar behavior, although in the case of solid GAP a higher fluence has been applied. For a given fluence, all liquid samples have comparable shock wave velocities (other fluences not shown), although the splashing behavior can be different.

Two elements here are *a priori* surprising. First, we could expect a difference in the shock wave velocity when a different splashing behavior is observed, but apparently, it is not the case. This fact have been also observed by Hopp and coworkers [21]. Therefore, the shock wave velocity is not a criterion to identify the nonsplashing conditions. Moreover, the timescale of the shock wave creation and propagation is much shorter than the time needed to observe splashing. This suggests that these two processes are independent of each other to a certain extent.

Secondly, the concentration of energetic material in the targets should yield a different shock wave velocity, which is not the case. The origin of this behavior in not yet understood. A tentative explanation could be that the shock wave is generated by molecules moving faster than the molecules in the atmosphere. In the case of solutions this is caused by the solvent molecules, explaining why it is the same for all concentrations. In the case of solid GAP no solvent molecules are available, and the material creating the shock wave comes from the decomposition of the polymer, which requires more energy supply than the vaporization of a liquid target. These results are supported by previous data [22], which shows that energetic polymer with very different decomposition enthalpies also show only very minor differences in the shock wave evolution.

3.3 SEM analysis

It was shown previously that the dispersion state of doping material has a large influence on the ablation crater morphology in solid samples [23], probably due to the inhomogeneity in the light absorption and subsequent material removal. A comparable influence is expected for liquid samples. To investigate this, the carbon particles size distribution in the solutions were analysed by wet scanning electron microscopy (WSEM).

In Fig. 7, we present backscatter images of the 0 and 1% GAP solutions. The brighter and darker regions repre-

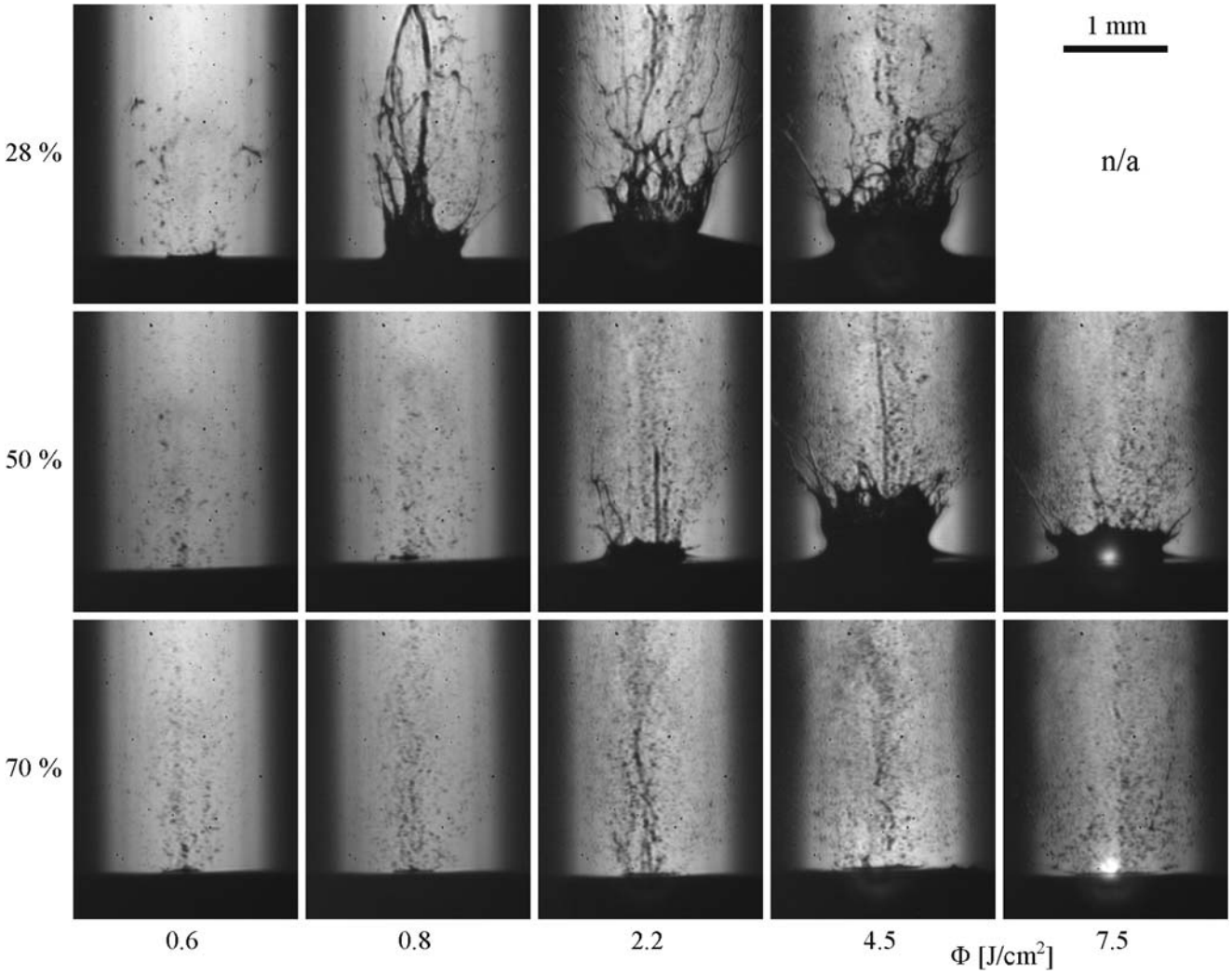

Fig. 5 Pictures taken after 10 µs for increasing GAP concentrations (*top* to *bottom*) and increasing fluences (from *left* to *right*). The transition from solid-like to splashing behavior is clearly visible

sent areas of higher and lower average atomic number, respectively. The distribution of CNP/CNP agglomerates are clearly visible in the suspension, where the uniform dark regions represent areas of solvent and the lighter areas represent the CNP agglomerates and associated impurities. While the morphological features in the two solutions are similar, there appears to be a higher density of CNP agglomerates at 1%, as observed in Fig. 7. Imaging was also performed with a 28% GAP solution as shown in Fig. 8, where the three solutions are compared at a larger magnification. A dramatic decrease in CNP agglomerate size is shown in Fig. 8c, on the order of 150–200 nm, in sharp contrast to the 2–10 µm features observed in the 0 and 1% solutions. Optical microscopy (not shown) reveals significantly larger CNP agglomerate size in solid GAP films, in the order of 20–100 µm. The domain in-between is experimentally not available because solutions with higher GAP concentrations decompose upon SEM exposure. The trend of the agglomerate size is a decrease with increasing GAP content in solution and an increase back in solid. As suggested previously [23], the distribution of the particles has an influence on the quality of the ablation crater and on the presence of particles in the ablation plume. The finer the dispersion, the more homogeneously light is absorbed and an ablation occurs. The formation of droplets may be prevented as well by a fine dispersion of the particles and thus a homogeneous absorption of the laser pulse.

The intensity of the backscattered signal is not a good indicator of the elemental composition, since it can either increase [24] or decrease [25] with increasing atomic number. Therefore, another method is preferred to investigate the composition. Energy dispersive X-ray analysis (EDX) was performed in *spot mode*, allowing to collect data on specific locations. Three points of reference were chosen from a 1% GAP solution based on backscatter image contrast, depicted as regions 1, 2 and 3 in Fig. 8b. The corre-

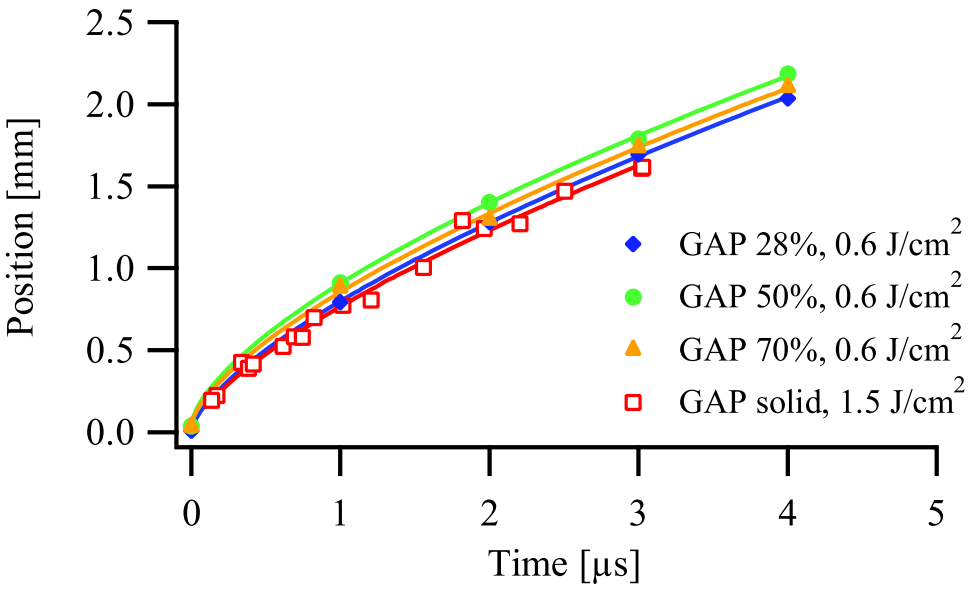

Fig. 6 Position of the shock wave versus time for different samples. The *solid lines* are guides for the eyes

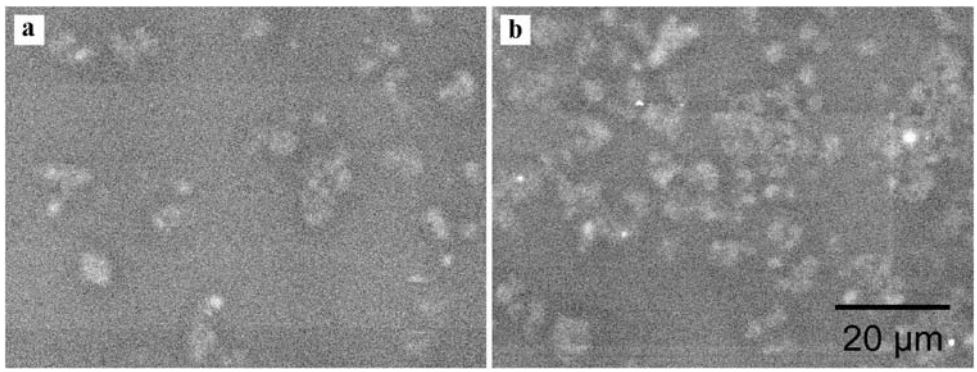

Fig. 7 SEM pictures of the 0 (**a**) and 1% (**b**) GAP solutions at the same magnification

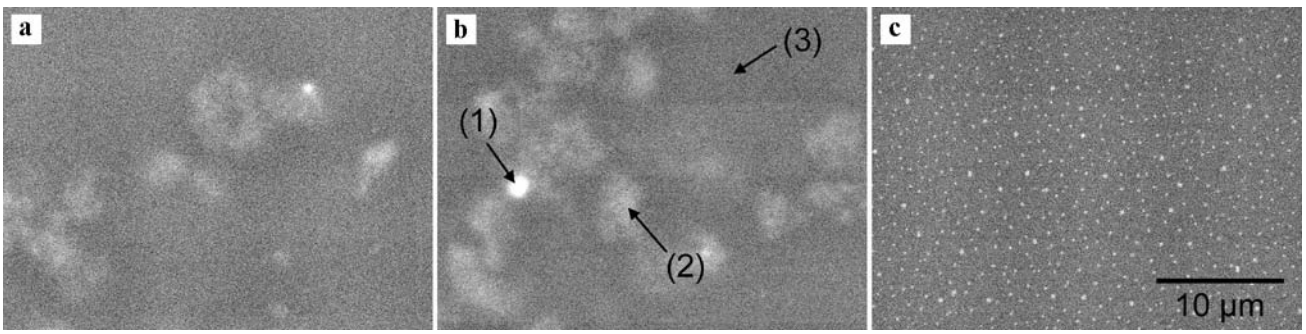

Fig. 8 SEM pictures of the 0 (**a**), 1 (**b**) and 28% (**c**) GAP solutions (magnified relative to Fig. 7). The *arrows* on (**b**) indicate where the EDX spectra shown in Fig. 9 were recorded

sponding spectra are presented in Fig. 9. Emission from the bright particle suggest it is rich in Ca (curve 1), in comparison to regions rich in C for both the CNP agglomerate and void areas (curves 2 and 3). As shown previously [23], Ca is present as impurity in the carbon nanoparticles: Ca evidence was detected by emission spectroscopy of ablated GAP + CNP films, while films of GAP doped with an infrared dye do not exhibit the Ca lines. Therefore, the presence of Ca shows that these clumps corresponds to CNP particles. Spectra from spot 1 and 2 show that calcium is not detected in every clump. This is probably due to an inhomogeneous CNP powder used, where not all particles contains Ca. The EDX results are in strong agreement with the conclusions drawn from the backscatter images and show that

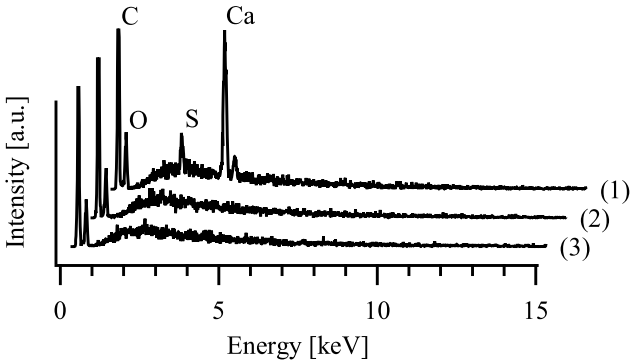

Fig. 9 EDX spectra of the 1% GAP solution recorded at three different locations (indicated on Fig 8). The *symbols* denote the elements (all Kα1 line)

the investigated solutions have different CNP sizes and dispersion states.

3.4 Preliminary thrust measurements

The 70% GAP solution is the most promising candidate as fuel for laser plasma thrusters. To assess this fact, preliminary thrust measurements were performed with a solution where the carbon particles were replaced by an infrared dye, to avoid plugging the exhaust nozzle by solid particles. Although the results may differ, this gives a good estimation of the performances of the system. The specific impulse of the 70% GAP + CNP solution was measured to be 680 s [26], which is even higher than the 250 s obtained for solid GAP doped with infrared dye [9]. The thrust measurements were done in vacuum to assess the ability of using liquid, i.e., volatile fuels in space. During the measurement time (about 30 min), the evaporation rate was found to be vanishing. Further measurement with carbon nanoparticles are in progress, but this clearly suggests that a viscous enough solution can be applied as fuel in micro laser plasma thrusters.

4 Conclusions

We have shown that suitable conditions can be found for using liquid GAP solution as fuel for micro laser plasma thrusters. The splashing behavior is controlled by the viscosity of the solution and the laser fluence, both determining a maximum amount of liquid displacement that should not be exceeded to avoid splashing. While imaging of the process is a very valuable tool for finding the appropriate conditions, the shock wave velocity is independent of the concentration for a given fluence and cannot be used as an indicator of the ablation regime. Finally, we showed that the dopant dispersion is different for the investigated GAP concentrations, which may have a important influence on the homogeneity of energy absorption and therefore on the ablation behavior of the liquid GAP solutions.

Acknowledgements Financial support from the Swiss National Science Foundation is gratefully acknowledged. Part of the effort was sponsored by the Air Force Office of Scientific Research, Air Force Material Command, USAF, under grant number FA8655-03-1-3058 and under contract order number FA8655-07-M-4015, and by the US National Science Foundation through grant DMII-0422632. We would like to thank Matthias Nagel and Frank Winnefeld for the viscosity measurement and Sebastian Heiroth for the preparation of GAP solutions.

References

1. C. Phipps, J. Luke, AIAA J. **40**, 310 (2002)
2. C. Phipps, J. Luke, G. McDuff, T. Lippert, Appl. Phys. A **77**, 193 (2003)
3. C. Phipps, J. Luke, T. Lippert, M. Hauer, A. Wokaun, J. Propuls. Power **20**, 1000 (2004)
4. C. Phipps, J. Luke, T. Lippert, M. Hauer, A. Wokaun, Appl. Phys. A **79**, 1385 (2004)
5. L. Urech, T. Lippert, C.R. Phipps, A. Wokaun, Appl. Surf. Sci. **253**, 6409 (2007)
6. C. Phipps, J. Luke, Laser space propulsion, in *Laser Ablation and its Application*, edn. by C. Phipps. Optical Sciences, vol. 129, 1st edn. (Springer, Berlin, 2007), pp. 407–434
7. W. Schall, H.-A. Eckel, W. Bohn, Laser propulsion thrusters for space transportation, in *Laser Ablation and its Application*, edn. by C. Phipps. Optical Sciences, vol. 129, 1st edn. (Springer, Berlin, 2007), pp. 435–454
8. L. Urech, T. Lippert, Designed polymers for laser ablation, in *Laser Ablation and its Application*, ed. by C. Phipps. Optical Sciences, vol. 129, 1st edn. (Springer, Berlin, 2007), pp. 281–297
9. L. Urech, T. Lippert, C.R. Phipps, A. Wokaun, Appl. Surf. Sci. **253**, 7646 (2007)
10. T. Yabe, C. Phipps, M. Yamaguchi, R. Nakagawa, K. Aoki, H. Mine, Y. Ogata, C. Baasandash, M. Nakagawa, E. Fujiwara, K. Yoshida, A. Nishiguchi, I. Kajiwara, Appl. Phys. Lett. **80**, 4318 (2002)
11. T. Yabe, S. Uchida, Laser propulsion, in *Laser Ablation and its Application*, ed. by C. Phipps. Optical Sciences, vol. 129, 1st edn. (Springer, Berlin, 2007), pp. 55–471
12. Y. Zhang, X. Lu, Z.Y. Zheng, F. Liu, P.F. Zhu, H.M. Li, Y.T. Li, Y.J. Li, J. Zhang, Appl. Phys. A **91**, 357 (2008)
13. Y. Tsuboi, H. Fukumura, H. Masuhara, Appl. Phys. Lett. **64**, 2745 (1994)
14. Y. Tsuboi, H. Fukumura, H. Masuhara, J. Phys. Chem. **99**, 10305 (1995)
15. A. Vogel, V. Venugopalan, Chem. Rev. **103**, 577 (2003). In special folder
16. I. Apitz, A. Vogel, Appl. Phys. A **81**, 329 (2005)
17. J. Li, J. Fitz-Gerald, J. Oberhauser, Appl. Phys. A **87**, 97 (2007)
18. I. Barshack, J. Kopolovic, Y. Chowers, O. Gileadi, A. Vainshtein, O. Zik, V. Behar, Ultrastruct. Pathol. **28**, 29 (2004)
19. I. Barshack, S. Polak-Charcon, V. Behar, A. Vainshtein, O. Zik, E. Ofek, M. Hadani, J. Kopolovic, D. Nass, Ultrastruct. Pathol. **28**, 255 (2004)
20. A. Nyska, C. Cummings, A. Vainshtein, J. Nadler, N. Ezov, Y. Grunfeld, O. Gileadi, V. Behar, Toxicol. Pathol. **32**, 357 (2004)
21. B. Hopp, T. Smausz, E. Tombácz, T. Wittmann, F. Ignácz, Opt. Commun. **181**, 337 (2000)
22. M. Hauer, D.J. Funk, T. Lippert, A. Wokaun, Thin Solid Films **453–454**, 584 (2004)
23. L. Urech, M. Hauer, T. Lippert, C. Phipps, E. Schmid, A. Wokaun, I. Wysong, Proc. SPIE Int. Soc. Opt. Eng. **5448**, 52 (2004)

24. J. Goldstein, A. Romig, D. Newbury, C. Lyman, P. Echlin, C. Fiori, D. Joy, E. Lifshin, *Scanning Electron Microscopy and X-Ray Microanalysis*, 2nd edn. (Plenum Press, New York, 1994)
25. P. Merli, V. Morandi, F. Corticelli, Ultramicroscopy **94**, 89 (2003)
26. C.R. Phipps, J.R. Luke, W. Helgeson, Laser-powered multi-newton thrust space engine with variable specific impulse, in *High-Power Laser Ablation VII* (Taos, NM, USA, SPIE, Bellingham, 2008), pp. 70051X–8